

Uranium-Contaminated Soils: Ultramicrotomy and Electron Beam Analysis*

by

E. C. Buck, N. L. Dietz, J. K. Bates, and J. C. Cunnane

Chemical Technology Division
ARGONNE NATIONAL LABORATORY
9700 South Cass Avenue
Argonne, IL 60439-4837

The submitted manuscript has been authored by a contractor of the U. S. Government under contract No. W-31-109-ENG-38. Accordingly, the U. S. Government retains a nonexclusive, royalty-free license to publish or reproduce the published form of this contribution, or allow others to do so, for U. S. Government purposes.

February 1994

*Work supported by the U.S. Department of Energy, Office of Technology Development, as part of the Uranium in Soils Integrated Demonstration Program, under contract W-31-109-ENG-38.

DISTRIBUTION OF THIS DOCUMENT IS UNLIMITED

DISCLAIMER

This report was prepared as an account of work sponsored by an agency of the United States Government. Neither the United States Government nor any agency thereof, nor any of their employees, make any warranty, express or implied, or assumes any legal liability or responsibility for the accuracy, completeness, or usefulness of any information, apparatus, product, or process disclosed, or represents that its use would not infringe privately owned rights. Reference herein to any specific commercial product, process, or service by trade name, trademark, manufacturer, or otherwise does not necessarily constitute or imply its endorsement, recommendation, or favoring by the United States Government or any agency thereof. The views and opinions of authors expressed herein do not necessarily state or reflect those of the United States Government or any agency thereof.

DISCLAIMER

Portions of this document may be illegible in electronic image products. Images are produced from the best available original document.

Uranium-Contaminated Soils: Ultramicrotomy and Electron Beam Analysis

E. C. Buck, N. L. Dietz, J. K. Bates, and J. C. Cunnane

Chemical Technology Division
Argonne National Laboratory
9700 South Cass Avenue
Argonne, IL 60439-4837

KEY WORDS: Ultramicrotomy, transmission electron microscopy, uranium, soils

ABSTRACT

Uranium-contaminated soils from the U.S. Department of Energy (DOE) Fernald Site, Ohio, have been examined by a combination of scanning electron microscopy with backscattered electron imaging (SEM/BSE) and analytical electron microscopy (AEM). The inhomogeneous distribution of particulate uranium phases in the soil required the development of a method for using ultramicrotomy to prepare transmission electron microscopy (TEM) thin sections of the SEM mounts. A water-miscible resin was selected that allowed comparison between SEM and TEM images, permitting representative sampling of the soil. Uranium was found in iron oxides, silicates (soddyite), phosphates (autunites), and fluorite (UO₂). No uranium was detected in association with phyllosilicates in the soil.

INTRODUCTION

The Fernald Feed Materials Production site in Ohio was engaged in uranium processing operations for 40 years. During this time, numerous uranium product spills and waste from a site incinerator contaminated the site. The U.S. Department of Energy (DOE) suspended production there in 1986 and is now involved in remediation of the site, which has now been termed the Fernald Environmental Management Project (FEMP) (Lee and Marsh, 1992). The soil at Fernald generally was contaminated by three sources: airborne uranium dust particles, aqueous uranium wastes, and solid uranium product spills. An extensive sampling program has identified the areas of major contamination and current efforts are focused on further analysis of selected samples. The collected soil samples contain between 100 and 500 ppm uranium. The basic components of the contaminated soils have been identified by scanning electron microscopy (SEM) and X-ray diffraction as various layer silicates and quartz. These examinations also revealed that uranium inclusions were associated with the clay fraction of the soil, but they did not yield a unique description of the phases.

We needed a method of locating uranium-bearing particles within a relatively large volume of soil. SEM with backscattered electron imaging ((SEM/BSE) was used

DISTRIBUTION OF THIS DOCUMENT IS UNLIMITED

at

MASTER

to locate particles; however, to identify these particles, samples suitable for transmission electron microscopy (TEM) of the uranium-bearing particle had to be made. This required the use of an embedding resin that had good infiltration properties for producing samples for observation in the SEM and that could also be sectioned by ultramicrotomy into electron-transparent samples for TEM. The combination of SEM and TEM would also allow both representative sampling of the soil and accurate structural identification of the submicron-sized uranium-bearing particles.

This paper (a) describes a method for preparing TEM samples of uranium-bearing soils and (b) describes the use of a combination of SEM/BSE for locating and characterizing micron-sized particles within radionuclide-contaminated soils. In addition to electron beam methods of analysis, other analytical techniques are being used to characterize the soil, including X-ray absorption spectroscopy and luminescence spectroscopy. These techniques complement one another, though given the nature of the distribution of uranium in the soil samples, AEM has been found to be extremely effective for determining the structure of the contaminant phases.

EXPERIMENTAL PROCEDURE

Uranium-bearing phases were isolated by using micromanipulation techniques, assisted by a Zeiss polarizing light microscope and a ISI SS-40 SEM that was equipped with a Robinson BSE detector. Thin sections for TEM analysis were produced with a Reichert-Jung Ultracut E ultramicrotome. The thin sections were collected on slotted, 150-mesh carbon-coated copper grids. AEM was performed using a JEOL 2000FXII TEM, operated at 200 kV. Compositional analysis was carried out by using an ultra-thin-window light element detector and high take-off angle beryllium window detector energy dispersive X-ray (EDS) detectors.

Phases were analyzed by using EDS and electron diffraction; selected area electron diffraction (SAED), and convergent beam electron diffraction (CBED). Electron diffraction data from uranium-bearing phases were compared to XRD data from the literature to assist in identification. The camera lengths for SAED were determined by using a polycrystalline aluminum standard. Because of the small size of many of the phases present in the soils, microdiffraction and CBED were often used to obtain structural data.

An important aspect of the overall analysis was the development of a technique for following a unique particle through each step in the analysis procedure. The main focus of the techniques was on the use of ultramicrotomy in preparing TEM sections.

ULTRAMICROTOMY

TEM thin-sectioning of isolated small particulates by ultramicrotomy is well described in the literature (Hayat, 1989; Kay, 1965). Thin sections of soil constituents have been prepared using ultramicrotomy, but the technique has seen limited use in

gross soil studies (Wada et al., 1989; Ghabru et al., 1990). In studies where a representative sample of the bulk is required, it is necessary to show that one is observing the same regions as characterization proceeds from the optical microscope to the scanning and transmission electron microscopes. This requires the use of a resin that is suitable for to optical and scanning electron microscope preparation and analysis and for ultramicrotomy of the sample for transmission electron microscopy. Comparison of SEM and TEM images from the same sample allows greater confidence in determining whether uranium-bearing phases are mere peculiarities or true representations of the contamination in the soil.

Preparation of TEM Thin Sections

To arrive at a representative characterization of uranium phases distributed in soil, a relatively large number of unaltered particles must be examined. This was achieved by mounting particles for SEM and examining polished cross sections with SEM/BSE. Because the uranium-containing particle is thin-sectioned directly from the SEM mount, the embedding resin must have optimum infiltration and sectioning properties. (Issues of resin selection are discussed below.) Particles were mounted either in inverted BEEM capsules (for small quantities) or in a suitable flat mold (for large quantities). Because a flat, shallow mold could be mounted in either the light microscope or the SEM, we were able to directly correlate the optical microscopy images and the SEM images. Selected uranium-bearing particles were identified in the SEM on the basis of morphological and compositional distinctions. Micrographs of regions containing uranium-bearing phases were taken and annotated, so that particles of interest could be examined in the polarizing optical microscope and used for TEM studies. In the flat molds, particles of interest were isolated for ultramicrotomy by scribing the resin around the particle and gluing this piece onto a sectioning block stub. In the inverted BEEM capsules, it was possible (when the particles were closely spaced) to shape two regions on the block face for simultaneous thin-sectioning.

Evaluation of Embedding Resins

Ultramicrotomy of soil particles is the most appropriate means of viewing the undisturbed spatial relationship of soil components. However, the success of this method depends on selecting the right resin, which can be problematic. The difficulty arises from the variety of soil components, each with differing mechanical properties, and from the requirements for producing a good section. Mechanical tests performed on a variety of embedding resins have helped clarify the relationship between resin properties and the forces involved in forming a thin section (Acetarin et al. 1987). The results of tensile and bending tests, combined with evaluation of thin sections, indicate that the best resin is one having a high elastic modulus and low plasticity. These characteristics favor a cleavage mechanism of sectioning, whereas a softer, more plastic resin favors true sectioning.

Section quality can be improved substantially by selecting a resin that has good cohesion and a hardness similar to that of the sample. Such a resin helps minimize sample heterogeneity, resulting in a more uniform thin section. Sectioning of the brittle, impenetrable components in the soils, such as quartz and uranium oxide

inclusions, can be optimized by determining the best microtome sectioning parameters, such as sectioning speed, cutting angle, and section thickness. Shattering of brittle phases is unavoidable, but good cohesion between particle and resin will usually hold some material at the interface, whereas poor cohesion would cause shattered pieces to be completely plucked out and redeposited over the surface of the section.

Because of the differences in resin properties and the large size distribution, heterogeneity, and anisotropy of the soil particles, it was necessary to evaluate several kinds of embedding media. The thermosetting epoxies commonly used in the preparation of TEM thin sections did not provide representative samples because they inadequately infiltrate the large particles and the clay fraction. An acrylic resin, miscible in ethanol and eight times less viscous than the epoxy, was used in a solvent replacement infiltration procedure. This procedure improved section quality considerably, but the sections did not show intact regions of the more compact structures and did not have satisfactory polishing characteristics or beam stability.

The best improvement in infiltration was achieved with a water-soluble melamine resin that was used to replace water in wetted soil particles. Frösch et al. (1985) compared sections made of the polar melamine resin and a nonpolar epoxide resin; their results showed that the melamine resin produced much thinner and smoother (i.e., low surface relief) thin sections. A rough surface indicates that a large amount of plastic work has taken place prior to rupture. Therefore, the smoother melamine sections, which underwent less plastic flow, required less energy for sectioning. With the melamine resin, less energy is required to break the bonds, and thin sections less than 10nm thick can reportedly be obtained. The particles were prepared following a procedure similar to that used to prepare aquatic colloids (Perret et al., 1991).

When melamine resin is used, SEM results show an improvement in the polished surface and in the infiltration of large particles. Because the spatial relationship of uranium phases within the larger particles was well preserved, more uranium-containing areas could be isolated in a given field of view. The increased section quality resulting from these improvements made it possible to produce completely intact sections that were thinner than sections obtained with epoxy and acrylic resins. Consequently, the uranium phases identified in the TEM could be correlated with the corresponding areas in the SEM/BSE image.

In Figure 1, structures from the same particle can be seen in both the SEM and the TEM micrograph. The slight discrepancy in particle morphology between the SEM and the TEM image is due to the sectioning process, which may occur over a depth of ~3 μm ; however, the overall structure of the particles is preserved.

ELECTRON BEAM ANALYSIS

Characterization of uranium-bearing phases involved the combination of SEM and AEM. Each of these techniques provided information which, in many instances, allowed complete characterization of the phases.

Soil samples from Fernald commonly contained uranium oxide particles (see Figure 2). It is difficult to section uranium oxide in the microtome, and often particles were scattered from their original positions. With the SEM images of the area we can, however, reconstruct the relationship of these phases to the rest of the soil component phases. The uranium oxide particles were found to possess a cubic fluorite structure, so they were identified as uraninite (UO_2). UO_2 is not observed in natural uranium deposits, because uraninite readily undergoes oxidization to a nonstoichiometric state (Finch and Ewing, 1992). No evidence of nonstoichiometry was found, although the sections were probably not thin enough for us to observe of any defect structure that might have been produced by the introduction of excess oxygen atoms into the uraninite lattice. Uranium oxide particles on the order of $>1 \mu\text{m}$ could normally be identified by SEM, once the TEM had been used to characterize a few particles in particular sample. However, uranium was occasionally associated with other phases, such as iron, giving the impression that the uranium was incorporated in another phase. TEM analysis was required to show that, in fact, the particle consisted of submicron-sized uranium oxide particles closely associated with nonuranium-bearing phase.

In other cases where uranium was found to be closely associated with another element, the uranium was found to be incorporated within another phase. Figure 3 shows an amorphous, uranium-bearing iron oxide phase from one soil sample (this is the uranium-bearing phase in Figure 1). The phase had a variable uranium content, which suggested that the uranium had been adsorbed onto the iron phase. In this example, the sectioning technique preserved the spatial relationship of the uranium-bearing particles to other phases in the soil. This information helps in determining how the uranium is being redistributed in the soils. These types of phases could not be uniquely identified during SEM analysis and always required TEM confirmation.

It was thought that most of the contamination at Fernald took the form of uranium oxide, but we have found that uranium has been incorporated into other phases. The presence of these phases suggests that uranium has undergone weathering processes (i.e., that it has been redistributed in the soil). Nearly all of the soils from the various sampling sites around Fernald were found to contain uranium phosphate phases. These phases, consisting of long, fibrous particles, were identified on the basis of electron diffraction patterns (Figure 4) as a tetragonal meta-autunite: uranyl phosphate hydrate, ideally $[\text{M}^{2+}(\text{UO}_2)_2(\text{PO}_4)_2 \cdot x\text{H}_2\text{O}]$. These phases are extremely beam-sensitive, going amorphous after only a short exposure to the beam. Structural identification of the uranium-bearing phase also indicates that the uranium is in the uranyl state $[\text{U}(\text{VI})]$. Furthermore, apatite (calcium phosphate) was present in the same region, a result made possible because the technique preserves the spatial relationships among phases.

Uranium phosphates are highly insoluble phases, which are well-known as alteration products of uraninite (Finch and Ewing, 1992). In geological deposits, uraninite can alter through nonstoichiometric oxidation, forming of three types of uranium phases: gummities (e.g., schoepite), autunites (uranium phosphates), and uranophanes (e.g., boltwoodite), depending on the solution conditions (Finch and

Ewing, 1992; Wronkiewicz et al., 1992). However, given the time for reaction at Fernald, it is more likely that autunites were formed by the interaction of soluble uranium from spills at the plant with phosphate in solution released from apatite minerals in the soil (Buck et al., 1994b). The uranium phosphate phases had a distinctive morphology which could be recognized in the SEM. Once this phase had been identified in the AEM, its concentration in the soil samples could be estimated purely on the basis of SEM observation.

Another possible alteration phase, uranium silicate was identified one Fernald site soil sample. The d spacings calculated from the electron diffraction from this phase, which are displayed in Table I, were consistent with soddyite, ideally $[(\text{UO}_2)_2(\text{SiO}_4) \cdot 2\text{H}_2\text{O}]$, a uranyl silicate. This phase has been commonly found as an alteration product in both laboratory-reacted and field-weathered uraninite (Wronkiewicz et al., 1992; Finch and Ewing, 1992). It has a high uranium-to-silicon ratio, which distinguishes it from other uranium silicates (Stohl and Smith, 1981). The phase was found sandwiched between phyllosilicate minerals (Figure 5) which suggests that discrete uranium phases may be forming in the soil preferentially, rather than undergoing adsorption onto other soil phases. This type of uranium-bearing phase could not be resolved in the SEM, and it was rare enough that it could not be readily identified in the SEM.

In addition to the uranium-bearing phases, the following nonuranium-bearing phases were identified in the Fernald soil: (in order of decreasing amount: quartz, clay, calcite, dolomite, apatite, illmentite, as well as particles of cerium phosphate, zircon, and yttrium phosphate. The presence of many of these phases will affect the mobility of uranium in the soils.

DISCUSSION

The application of SEM and AEM can provide a clearer picture of uranium contamination at Fernald. In the technique described a uranium-rich region is located by SEM, a thin section is produced from that region by ultramicrotomy, and TEM analysis is used to characterize the structure accurately by analyzing the composition of the uranium-bearing phase. If this technique is not used, AEM identifications will be random and infrequent and SEM analysis will be inaccurate and ineffective for determining phase structure.

The presence of autunite and soddyite phases suggests that some of the weathering processes at Fernald have resulted in the alteration of the initial uranium-bearing phases and that soluble uranium interacted only slightly with the clay phases in the soil substrate. This conclusion is based on the application of EDS compositional analysis, (0.1 wt% detection limit): no uranium was found associated with the clay phases in the soil.

Effective removal of uranium from the Fernald soils will depend on detailed knowledge of the chemical and physical characteristics of the waste and its environment.

Without information describing the nature of the uranium contamination, remediation technologies must operate by trial and error, which may result in repetitive processing and an even greater volume of contamination than was initially present. The characterization methods described above, in combination with other methods under development, will allow remediation technology groups to find a more direct and efficient way of removing the contamination. These techniques are intended to be transferred for implementation at contaminated sites operated by DOE and private sector. For example, similar techniques could be applied to plutonium contamination at Johnston Atoll (Bramlitt, 1988), Hanford (Cleveland, and Rees, 1981), and Maxey Fats (Sheppard, 1979).

ACKNOWLEDGMENT

This work was supported by the U.S. Department of Energy, Office of Technology Development, as part of the Uranium in Soils Integrated Demonstration Program, under contract W-31-109-ENG-38.

REFERENCES

- Acetarin, J-D., Carlemalm, E., Kellenberger, E., and Villiger, W. (1987) *J. Elect. Micro./Tech.* 6: 63.
- Bramlitt, E. T. *Health Physics* (1988) 55: 451-453
- Buck, E. C., Cunnane, J. C., Bates, J. K., and Dietz, N. L. (1993) *AEM of Uranium Contaminated Soils from the DOE Fernald Operation Site, Proceedings of Waste Management '93, Tucson, AZ* 978.
- Buck, E. C., Brown, N. R. and Dietz, N. L., *Distribution of Uranium Phases in Fernald Soils, Mat. Res. Soc. Symp. Proc., 333 Boston* (1994).
- Cleveland, J .M. and Rees, T. F. (1981) *Science* 212: 1506.
- Cunnane, J. C., Lee, S. Y., Perry, D. L. Tidwell, V. C., Gill, V.. and Mickelson, M. (1993) *Proceedings of Waste Management '93, Tuscon, AZ.*
- Edghill, R. (1991) *Radiochimica Acta* 52/53: 381-386.
- Finch, R. J. and Ewing, R. C. (1992) *J. Nuc. Mat.* 190: 133-156.
- Frösch, D., Westphal, C., and Bachhuber, K. (1988) *Ultramicroscopy* 17: 141.
- Ghabru, S. K., Mermut, A. R. and St. Arnaud, R. J.; (1990) *Soil. Sci. Soc. Am. J.* 54: 281.
- Hayat, M. A. Principles and Techniques of Electron Microscopy: Biological

- Applications, 3rd ed., CRC Press, Inc., Boca Raton, FL (1987).
- Kay, D. Techniques for Electron Microscopy. Blackwell Press, Oxford (1965).
- Lee, S. Y. and Marsh, J. D. ORNL/TM-11980, Oak Ridge National Laboratory, Oak Ridge, TN (1992).
- Perret, D., Leppard, G. G., Müller, M., Belzile, N., de Vitre, R., and Buffle, J. (1991) *Water Research* 25: 1333-1343.
- Sheppard, J. C., Campbell, M. J., Kittrick, J. A., and Hardt, T. L. (1979) *Environmental Science and Technology* 13: 680-684.
- Stohl, F.V. and Smith, D.K. (1981) *American Mineralogist* 66: 610-624.
- Wada, K. and Kakuto, W. (1990) *Clays and Clay Minerals* 37: 263.
- Wronkiewicz, D. J., Bates, J. K., Gerding, T. J., Veleckis, E., and Tani, B. S. J. *Nuc.Mat.* (1992) 192: 107-127.

DISCLAIMER

This report was prepared as an account of work sponsored by an agency of the United States Government. Neither the United States Government nor any agency thereof, nor any of their employees, makes any warranty, express or implied, or assumes any legal liability or responsibility for the accuracy, completeness, or usefulness of any information, apparatus, product, or process disclosed, or represents that its use would not infringe privately owned rights. Reference herein to any specific commercial product, process, or service by trade name, trademark, manufacturer, or otherwise does not necessarily constitute or imply its endorsement, recommendation, or favoring by the United States Government or any agency thereof. The views and opinions of authors expressed herein do not necessarily state or reflect those of the United States Government or any agency thereof.

Table I. Electron diffraction data on uranium silicate phase

Experimental d spacings (Å)	\pm (Å) ^a	Soddyite
6.41	0.14	6.296
4.89	0.09	4.805
4.53	0.08	4.56
3.79	0.06	3.803
3.38	0.05	3.348
2.75	0.04	2.720
2.65	0.04	2.657
2.52	0.04	2.52 ^b
2.32	0.03	2.335
1.88	0.03	1.864
1.77	0.02	1.772

^aErrors are based on the inaccuracies associated with the measurement of the spacings and instrument instability.

^bReflection observed in synthetic hydrated uranyl silicate (Stohl and Smith, 1981).

FIGURE CAPTIONS

- Fig. 1. SEM/BSE micrographs (a) showing soil particles, which can also be seen in the TEM image (b). The uranium-contaminated regions can be identified by the white BSE contrast. The particles are similar in shape because the SEM mount has been sectioned nearly parallel to the plane of the paper (the arrows point to the same spot on the SEM and TEM images).
- Fig. 2. AEM analysis of uranium oxide particles found in soil samples from Fernald, electron diffraction patterns taken along the (a) $\langle \bar{1}10 \rangle$ and (b) $\langle 100 \rangle$ zone axis (b) micrograph of uranium oxides particles in soil sample.
- Fig. 3. TEM micrograph of an amorphous iron oxide phase which contained clumps of uranium-rich iron oxide particles. The feature at the top right is a fold in the epoxy.
- Fig. 4. (a) TEM image of a tetragonal autunite, uranyl phosphate hydrate, identified by (b) SAED taken down the $\langle 001 \rangle$ zone axis and (c) EDS analysis. Note that the $\text{Cu-K}_{\alpha,\beta}$ peaks are due to fluorescence from the copper support grid.
- Fig. 5. A uranium-rich silicate phase was found between chlorite, and phyllosilicate phases, (a) and identified as ooddyite $[(\text{UO}_2)_2\text{SiO}_2 \cdot 2\text{H}_2\text{O}]$, a uranyl silicate, by electron diffraction (see Table I) and (b) EDS compositional analysis.

Fig. 1. (a) SEM/BSE micrographs showing soil particles, which can also be seen in the (b) TEM image. The uranium-contaminated regions can be identified by the white BSE contrast. The particles are similar in shape because the SEM mount has been sectioned nearly parallel to the plane of the paper (the arrows point to the same spot on the SEM and TEM images).

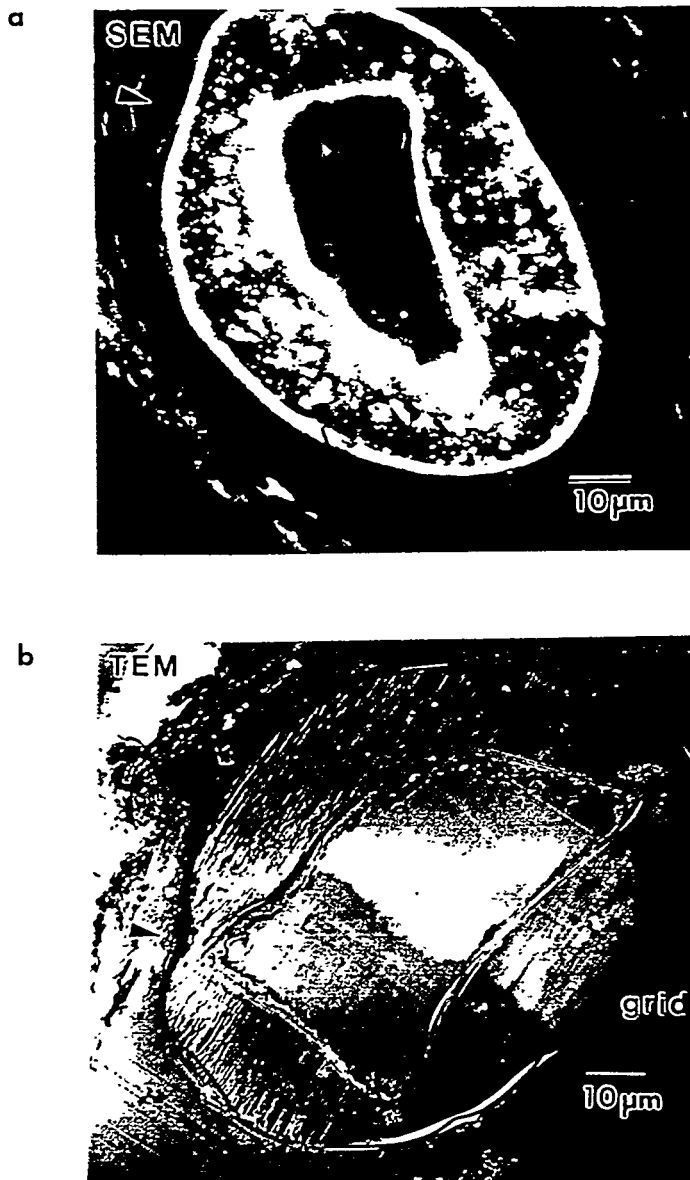


Fig. 2 AEM analysis of uranium oxide particles found in soil samples from Fernald, taken along the (a) $\langle \bar{1}10 \rangle$ and (b) $\langle 100 \rangle$ beams directions, (b) micrograph of uranium oxides particles in soil sample.

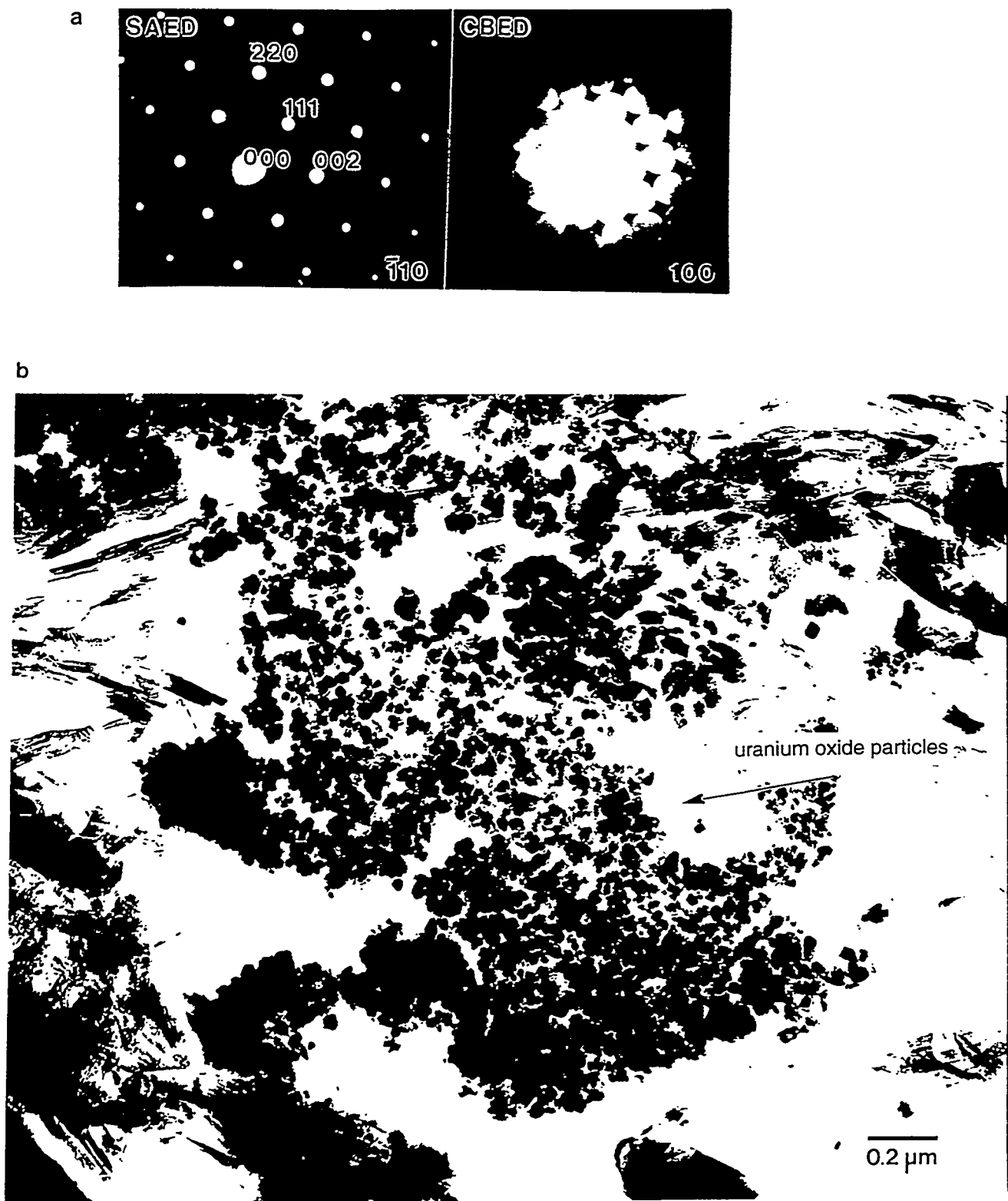


Fig. 3. TEM micrograph of an amorphous iron oxide phase which contained clumps of uranium-rich iron oxide particles. The feature in the top right is a fold in the epoxy.

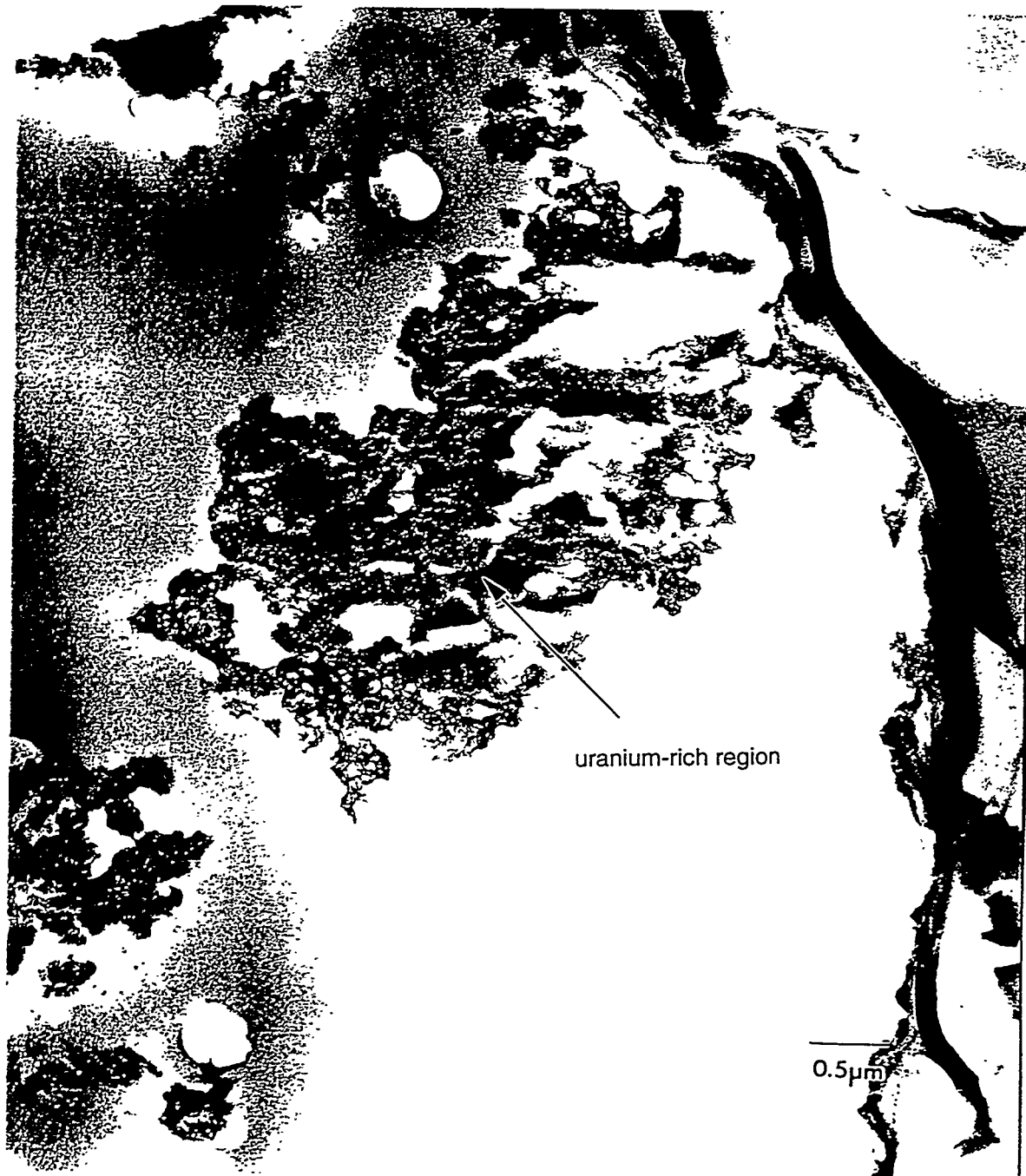


Fig. 4. (a) TEM image of a tetragonal autunite, uranyl phosphate hydrate, identified by (b) SAED taken down the $\langle 001 \rangle$ zone axis, and (c) EDS analysis.

N.B. the $\text{Cu-K}_{\alpha\beta}$ peaks are due to fluorescence from the copper support grid.

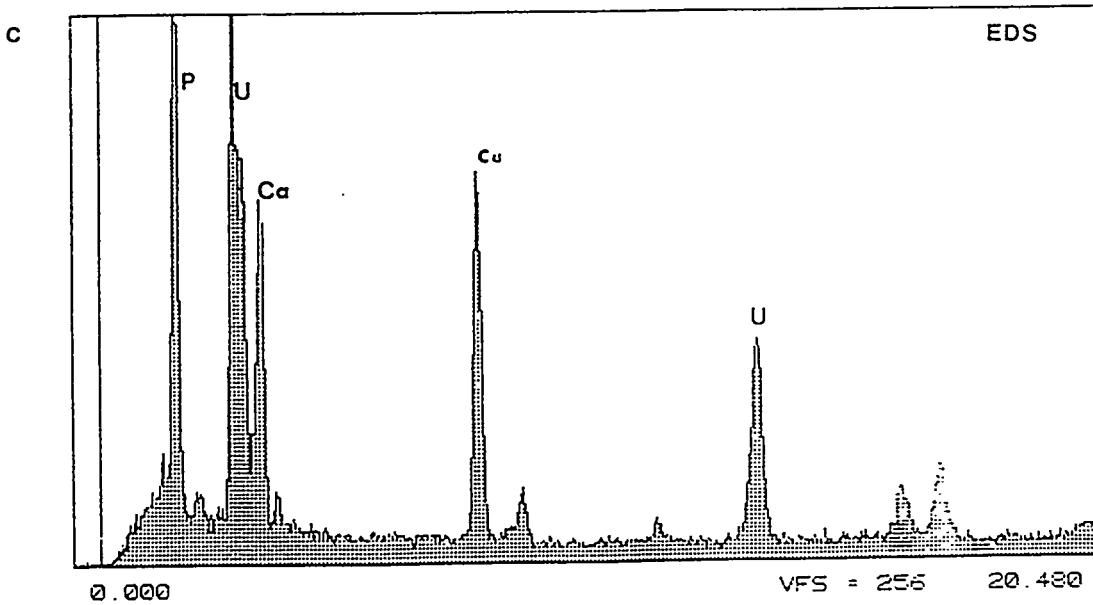
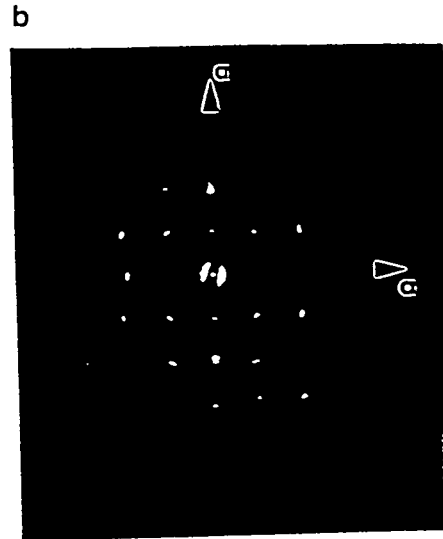


Fig. 5. Between chlorite, phyllosilicate phases, a uranium-rich silicate phase was found (a) and identified as the uranyl silicate, soddyite $[(\text{UO}_2)_2\text{SiO}_2 \cdot 2\text{H}_2\text{O}]$ by electron diffraction (see Table I) and (b) EDS compositional analysis.

